Am J Physiol Heart Circ Physiol 295: H1743–H1752, 2008.
First published August 22, 2008; doi:10.1152/ajpheart.00617.2008.

Formation and function of ceramide-enriched membrane platforms with CD38 during M_1-receptor stimulation in bovine coronary arterial myocytes

Su-Jie Jia,* Si Jin,* Fan Zhang, Fan Yi, William L. Dewey, and Pin-Lan Li

Department of Pharmacology and Toxicology, Medical College of Virginia, Virginia Commonwealth University, Richmond, Virginia

Submitted 11 June 2008; accepted in final form 20 August 2008

Jia SJ, Jin S, Zhang F, Yi F, Dewey WL, Li PL. Formation and function of ceramide-enriched membrane platforms with CD38 during M_1-receptor stimulation in bovine coronary arterial myocytes. *Am J Physiol Heart Circ Physiol* 295: H1743–H1752, 2008. First published August 22, 2008; doi:10.1152/ajpheart.00617.2008.—CD38 contains an ADP ribosylcyclase domain that mediates intracellular Ca^{2+} signaling by the production of cyclic ADP-ribose (cADPR), but the mechanisms by which the agonists activate this enzyme remain unclear. The present study tested a hypothesis that a special lipid-raft (LR) form, ceramide-enriched lipid platform, contributes to CD38 activation to produce cADPR in response to muscarinic type 1 (M_1) receptor stimulation in bovine coronary arterial myocytes (CAMs). By confocal microscopic analysis, oxotremorine (Oxo), an M_1 receptor agonist, was found to increase LR clustering on the membrane with the formation of a complex of CD38 and LR components such as GM_1, acid sphingomyelinase (ASMase), and ceramide, a typical ceramide-enriched macrodomain. At 80 μM, Oxo increased LR clustering by 78.8%, which was abolished by LR disruptors, methyl-β-cyclodextrin (MCD), or filipin. With the use of a fluorescence resonance energy transfer (FRET) technique, 15.5 ± 1.9% energy transfer rate (vs. 5.3 ± 0.9% of control) between CD38 and LR component, ganglioside M_1 was detected, further confirming the proximity of both molecules. In the presence of MCD or filipin, there were no FRET signals detected. In floated detergent-resistant membrane fractions, CD38 significantly increased in LR fractions of CAMs treated by Oxo. Moreover, MCD or filipin attenuated Oxo-induced production of cADPR via CD38. Functionally, Oxo-induced intracellular Ca^{2+} release and coronary artery constriction via cADPR were also blocked by LR disruption or ASMase inhibition. These results provide the first evidence that the formation of ceramide-enriched lipid macrodomains is crucial for Oxo-induced activation of CD38 to produce cADPR in CAMs, and these lipid macrodomains mediate transmembrane signaling of M_1 receptor activation to produce second messenger cADPR.

lipid microdomains; sphingolipid; lipid mediator; smooth muscle; calcium signaling

CYCLIC ADP-RIBOSE (cADPR), an alternative Ca^{2+} mobilizing second messenger to inositol 1,4,5-trisphosphate [Ins(1,4,5)P_3], has been indicated to participate in the regulation of many cell functions or physiological processes, including insulin secretion, egg fertilization, cell proliferation, nitric oxide-induced Ca^{2+} movement, lymphocyte activation, and neural activity (13, 37). Recent studies in our laboratory and by others have reported that in vascular smooth muscle, cADPR contributes to the Ca^{2+} release from the sarcoplasmic reticulum (SR) induced by Ins(1,4,5)P_3-independent agonists, such as acetylcholine, oxotremorine (Oxo), 5-hydroxytryptamine, angiotensin II, and endothelin, leading to the contraction of arterial smooth muscle via ryanodine receptor (RyR)-mediated intracellular Ca^{2+} release (5, 11, 26). This cADPR/RyR-mediated Ca^{2+} signaling is now recognized as a fundamental mechanism regulating vascular function. CD38 is one of the important enzymes responsible for the production and metabolism of cADPR in vascular cells, and therefore CD38/cADPR pathway is considered as an important signaling pathway in the regulation of vasomotor responses (32). It is believed that the activation of this enzyme participates, at least in part, in Oxo-induced vasoconstriction and other receptor-mediated agonist responses (21, 38). However, the precise mechanism by which CD38 is activated by various agonists still remains unclear. Since this enzyme has been shown to localize outside cells constitutively in many studies, it is very puzzling how this enzyme could produce an intracellular second messenger to exert its signaling action.

Recently, lipid-raft (LR) clustering on the cell membrane is emerging as a novel mechanism mediating the transmembrane signaling in response to various stimuli in a variety of cell types, including lymphocytes, endothelial cells, and neurons (15, 16, 41). It has been shown that clustered membrane LRs form membrane signaling platforms, in particular, the ceramide-enriched platforms or macrodomains. These lipid platforms may recruit or aggregate various signaling molecules such as trimeric G proteins, small G proteins, sphingomyelin (SM), tyrosine kinases, NADPH oxidase subunits, phosphatases, and many others, resulting in the activation of different signaling pathways. Recent studies have reported that LRs are closely associated with the CD38 pathway in various lymphocytes and these LRs may be responsible for endocytosis of CD38 and the activation of certain signaling pathways (35, 46). However, the identity of these LRs remains unclear, and it is also unknown whether LRs during its clustering are involved in cADPR-mediated Ca^{2+} signaling. In previous studies, a rapid activation and translocation of acid sphingomyelinase (ASMase) into LRs were observed in response to various stimuli such as FasL, TNF-α, and endostatin (29, 33, 41). Moreover, our previous work also demonstrated that lysosomal ASMase contributes to the formation of LR redox signaling platforms by hydrolyzing SM to produce ceramide, which produces ceramide-enriched macrodomains or LR platforms, ultimately resulting in endothelial dysfunction (18). Based on these observations, the present study was designed to test the hypothesis that ceramide-enriched LR platforms may mediate an agonist-induced transmembrane signaling of CD38 and thereby participate in

* S.-J. Jia and S. Jin contribute equally to this work.

Address for reprint requests and other correspondence: P.-L. Li, Dept. of Pharmacology and Toxicology, Medical College of Virginia Campus, Virginia Commonwealth Univ., 410 N. 12th St., Richmond, VA 23298 (e-mail: pli@vcu.edu).

The costs of publication of this article were defrayed in part by the payment of page charges. The article must therefore be hereby marked "*advertisement*" in accordance with 18 U.S.C. Section 1734 solely to indicate this fact.

Oxo-induced CD38 activation to produce cADPR in coronary arterial myocytes (CAMs). To test this hypothesis, we first characterized the formation of ceramide-enriched LR clusters in CAMs in response to Oxo. We then examined the role of this LR clustering in aggregation and activation of CD38 in the membrane of these cells and explored the related molecular mechanisms mediating Oxo-induced ceramide production and LR platforms formation via ASMase/ceramide pathway. Furthermore, we determined whether this ceramide-enriched signaling platform with activated CD38 contributes to Ca^{2+} release in CAMs, ultimately leading to the constriction of coronary arteries.

MATERIALS AND METHODS

Bovine hearts were purchased from a local slaughterhouse and were used to isolate coronary artery smooth muscle cells. No living animals were used for the present study, and therefore there was no concern over vertebrate animal use.

Cell culture. Bovine CAMs were cultured as described previously (3, 42–45). Briefly, coronary arteries dissected from bovine hearts were first rinsed with 5% FBS in medium 199 containing 25 mM HEPES with 1% penicillin, 0.3% gentamycin, and 0.3% nystatin and then cut into segments, and the lumen was filled with 0.4% collagenase in medium 199. After 30 min of incubation at 37°C, the arteries were flushed with medium 199. The strips of denuded arteries were placed into gelatin-coated flasks with medium 199 containing 10% FBS with 1% L-glutamine, 0.1% tylosin, and 1% penicillin-streptomycin. CAMs migrated to the flasks within 3–5 days. Once cell growth was established, the arteries were removed and growing CAMs were cultured in medium 199 containing 20% FBS. The identification of CAMs was based on positive staining by an anti-α-actin antibody. Cells of *passages 2–4* were used in the present study.

Confocal analysis of LR clusters in CAMs. Individual LRs are too small (~50 nm in diameter) to be resolved by standard light microscopy; however, if LR components are cross-linked in living cells, clustered raft protein and lipid components can be visualized by fluorescence microscopy. For microscopic detection of LR platforms, CAMs were grown on glass coverslips and then treated with different doses of Oxo (20–120 μM; Sigma, St. Louis, MO) for 15 min to induce clustering of LRs. In additional groups of cells, LR disruptors filipin (1 μg; Sigma) or methyl-β-cyclodextrin (MCD; 100 μM; Sigma) or an ASMase inhibitor desipramine (Des, 10 μM; Sigma) were added and incubated for 20 min before Oxo stimulation.

These cells were then washed in cold PBS and fixed for 10 min in 4% paraformaldehyde and blocked with 1% BSA in TBS for 30 min. GM_1 gangliosides enriched in LRs were stained by Alexa488-labeled cholera toxin B (Alexa488-CTXB, 1 μg/ml) (Molecular Probes, Eugene, OR). The stained cells were then extensively washed, fixed in 4% paraformaldehyde for another 10 min, and mounted on glass slide with Vectashield mounting media (Vector, Burlingame, CA). The staining of LRs was visualized using an Olympus scanning confocal microscope (Olympus, Tokyo, Japan) at excitation/emission of 495/519 nm. The patch or macrodomain formation of Alexa488-labeled CTX, namely, gangliosides complex, represents the clusters of LR. Clustering was defined as one or several intense spots or patches, rather than diffuse fluorescence on the cell surface, whereas a vast majority of unstimulated cells displayed a homogenous or diffuse distribution of fluorescence throughout the membrane. In each experiment, the presence or absence of clustering in 200 cells was independently scored by unwitting researchers after the criteria for positive spots of fluorescence were specified. Cells that displayed a homogenous distribution of fluorescence were indicated negative. Results were given as the percentage of cells showing one or more clusters after indicated treatments.

Colocalization of LR clusters and CD38, ASMase, or ceramide in CAMs. For dual-staining detection of the colocalization of LRs and ceramide or ASMase, CAMs were first incubated with Alexa488-labeled CTX as described in *Confocal analysis of LR clusters in CAMs* and then with mouse anti-ceramide IgM antibody (1:200; Alexis Biochemicals, San Diego, CA) or goat anti-ASMase antibodies (1:200; Santa Cruz, Santa Cruz, CA) separately in different groups of cells, which was followed by Cy3-conjugated anti-mouse or Texas red-labeled anti-goat (Molecular Probes, Eugene, OR) secondary antibody as needed, respectively.

Fluorescence resonance energy transfer measurement. To further determine the molecular complex in LR clusters, CAMs were stained with tetramethylrhodamine isothiocyanate (TRITC) -labeled CTXB and FITC-labeled anti-CD38 antibody and then visualized under a confocal microscope. An acceptor bleaching protocol was employed to measure the fluorescence resonance energy transfer (FRET) efficiency (31, 36). After the prebleaching images were normally taken, the laser intensity at an excitation wavelength of the acceptor (TRITC) was increased from 50 to 98 W/cm^2 and continued to excite the sample cells for 2 min to bleach the acceptor fluorescence. After the excitation intensity was adjusted back to 50 W/cm^2, the postbleaching image was then taken. The FRET images were obtained by the subtraction of the prebleaching image from the postbleaching image and shown in blue color. After the measurement of FITC fluorescence intensity in images acquired at pre- and postbleaching as well as the FRET images, a FRET efficiency was calculated through the following formula: $E = (FITC_{post} - FITC_{pre})/FITC_{post} \times 100\%$ as described previously (14), where FITC fluorescence intensity was obtained from labeling of CD38.

Assay of ASMase activity. The activity of ASMase in CAMs was determined as described in our previous studies (39). Briefly, homogenates from CAMs were centrifuged at 1,000 g for 10 min to remove cell nuclei, and 50 μl of the supernatant homogenate were used for enzyme activity analysis. The ASMase activity was measured using radiolabeled substrate, [*N*-methyl-^{14}C]-SM (Perkin-Elmer Life Sciences). The assay mixture contained 100 nmol of SM (1,154 dpm/nmol) in 100 mM sodium acetate (pH 5.0), 0.1% Triton X-100, and 0.1 mM EDTA. After incubation at 37°C for 1 h, the reaction was stopped by adding 1.5 ml of chloroform:methanol (2:1 vol/vol), followed by an addition of 0.2 ml of water. A portion of the aqueous phase was transferred to scintillation vials and counted in a liquid scintillation counter for radioactivity of the reaction product, [^{14}C]choline phosphate.

Floatation of membrane LR fractions. To isolate LR microdomain fractions from cell membrane, CAMs were lysed in 1.5 ml morpholinoethanesulfonic acid-buffered sample buffer containing (in μmol/l) 25 morpholinoethanesulfonic acid, 150 NaCl, 1 EDTA, 1 PMSF, and 1 Na_3VO_4 and a mixture of "complete" protease inhibitors and 1% Triton X-100 (pH 6.5). Cell extracts were homogenized by five passages through a 25-gauge needle. Homogenates were adjusted with 60% OptiPrep Density Gradient medium to 40% and overlaid with discontinuous 30% to 5% OptiPrep Density Gradient medium. Samples were centrifuged at 32,000 rpm for 30 h at 4°C using a SW32.1 rotor. Fractions were collected from top to bottom. For immunoblot analysis of LR-associated proteins, these fractions were precipitated by mixing with equal volume of 30% trichloroacetic acid and 30 min of incubation on ice. Precipitated proteins were spun down by centrifugation at 13,000 rpm at 4°C for 15 min. The protein pellet was carefully washed with cold acetone twice, air dried, and then resuspended in 1 mol/l Tris·HCl (pH 8.0), which was ready for immunoblot analysis.

Western blot analysis. For immunodetection of LR-associated proteins, 50 μl of resuspended proteins were subjected to SDS-PAGE, transferred onto a nitrocellulose membrane, and blocked as described previously (41). The membrane was probed with primary monoclonal antibodies of anti-flotillin-1 (1:1,000, a LR marker proteins; BD Biosciences, San Jose, CA), anti-CD38 (1:1,000, BD Biosciences), or anti-ASMase (1:1,000, Santa Cruz) overnight at 4°C, followed by an

incubation with horseradish peroxidase-labeled anti-mouse or anti-goat IgG (1:5,000). The immunoreactive bands were detected by chemiluminescence methods according to the manufacturer's instruction and visualized on Kodak Omat film. The intensity of the immunoreactive bands was quantified by densitometry.

HPLC analysis of ADP-ribosyl cyclase activity in CAMs. To determine ADP-ribosyl cyclase activity, homogenates from CAMs (100 μg protein) were incubated with 100 μM β-nicotinamide guanine dinucleotide (β-NGD^+) at 37°C for 90 min. β-NGD^+ was used as a substrate to determine ADP-ribosyl cyclase activity because this enzyme is able to convert NGD into cyclic GDP-ribose (cGDPR) at the same reaction efficiency as working to convert β-NAD^+ into cADPR, but cGDPR unlike cADPR may not be hydrolyzed by cADPR hydrolase. Therefore, the use of β-NGD^+ will maximally detect the production of this enzyme by the blockade of a further hydrolysis of its products. After the reaction, the mixtures were centrifuged at 4°C through an Amicon microultrafilter at 13,800 *g* to remove proteins, and then cGDPR was analyzed by HPLC with a fluorescence detector (Agilent 1100 series HPLC system and G1321aspectrofluorometer). The excitation wavelength of 300 nm and the emission wavelength of 410 nm were used to detect cGDPR produced via cADP-ribosyl cyclase. All HPLC data were collected and analyzed by an Agilent Chemstation. Nucleotides were resolved on a 3-μm Supelcosil LC-18 column (4.6 × 150 mm) with a 5-μm Supelcosil LC-18 guard column (4.6 × 20 mm, Supelco, Bellefonte, BA). The injection volume was 20 μl. The mobile phase consisted of 150 mM ammonium acetate (pH 5.5) containing 5% methanol (*solvent A*) and 50% methanol (*solvent B*). The solvent system was a linear gradient of 5% *solvent B* in *A* to 30% *solvent B* in *A* over 1 min, held for 25 min, and then increased to 50% *solvent B* over 1 min. The flow rate was 0.8 ml/min. Peak identities were confirmed by the comigration with known standards. Quantitative measurements were performed by the comparison of a known concentration of standards.

Measurement of intracellular Ca^{2+} concentration in CAMs. Determination of intracellular Ca^{2+} concentration in CAMs was performed to determine the contribution of LR-CD38 platforms to cADPR-mediated Ca^{2+} signaling. Briefly, CAMs were cultured on a glass coverslip to reach ~60–70% confluence, and the culture medium was then removed. The cells were next loaded with fura-2 acetoxymethyl ester (fura-2 AM, 5 μM; Molecular Probes) at 37°C for 30 min and incubated for 20 min to allow a complete hydrolysis of intracellular fura-2 AM to fura-2 in a Ca^{2+}-free Hanks' buffered saline solution containing (in mM) 137 NaCl, 5.4 KCl, 4.2 $NaHCO_3$, 3 Na_2HPO_4, 0.4 KH_2PO_4, 0.5 $MgCl_2$, 0.8 $MgSO_4$, 10 glucose, and 10 HEPES (pH 7.4). The coverslip was mounted horizontally on a Nikon Diaphoto TMD inverted microscope (Nikon, Japan). Oxo (80 μM) was added to the bath solution to induce Ca^{2+} release. This dose of Oxo was used in our several previous studies where muscarinic type 1 (M_1) receptor was activated and cADPR and related Ca^{2+} release were produced in CAMs (11, 38). To examine the specificity of Oxo and the role of LRs in Oxo-induced Ca^{2+} release, the cells were pretreated for 15 min with 8-bromo-cADPR (8-Br-cADPR, a cADPR antagonist at 30 μM), LR disruptors, filipin (1 μg) or MCD (100 μM), or an ASMase inhibitor, Des (10 μM), and then Oxo-induced Ca^{2+} release was redetermined. All these experiments were conducted in Ca^{2+}-free Hanks' buffer. A SPOT digital camera (SPOT RT Monochrome; Diagnostic Instruments) was used to record fura-2 fluorescence images. Metafluor imaging and analysis software (Universal Imaging) was used to acquire, digitize, and store the images.

Vascular reactivity in perfused small coronary arteries in vitro. Vascular reactivity in isolated perfused and pressurized small bovine coronary artery was measured as described previously (11). The intramural coronary arteries (<300 μm in diameter) were dissected from fresh cow hearts and assembled between two glass tips. After a 60-min equilibration period under the transmural pressure of 60 mmHg, Oxo (80 μM) was added to the bath solution to induce vasoconstriction. When Oxo-induced contraction reached a stable plateau, the internal diameters of the arteries were measured and recorded. To examine the contribution of ASM/ceramide and LR/CD38 pathway to Oxo-induced vasoconstriction, the arteries were pretreated for 20 min with one of the following compounds: nicotinamide (Nicot; 6 mM; an inhibitor of ADP-ribosyl cyclase), 8-Br-cADPR (30 μM; a cADPR antagonist), LR disruptors, MCD (100 μM), and filipin (1 μg), or an ASMase inhibitor, Des (10 μM). Oxo (80 μM) was added and the vasoconstrictor response was observed as described in the protocol without these components. The contractile responses to Oxo were expressed as the percent reduction in vascular internal diameters.

Statistics. Data are presented as means ± SE. Significant differences between and within multiple groups were examined using ANOVA for repeated measures, followed by Duncan's multiple-range test. Student's *t*-test was used to determine the significance of difference in two groups of experiments. $P < 0.05$ was considered statistically significant.

RESULTS

Cofocal microscopy of Oxo-induced LR clustering in CAMs. Figure 1*A* presents the typical fluorescent confocal microscopic images depicting Alexa488-CTX-labeled patches on the cell membrane of CAMs. Under the resting condition (control), there was only a diffuse fluorescent staining on the cell membrane, indicating a possible distribution of a single LR. When CAMs were incubated with Oxo, some large fluorescent dots or patches were detected on the cell membrane, indicating LR patches or macrodomains. Figure 1*B* summarized the effects of different doses of Oxo on the LR clustering by counting these LR clusters or patches. It was found that under control condition, CAMs displayed a small percentage with LR clustering (19.6 ± 3.9%). After these cells were stimulated with Oxo, LR-clustered positive cells increased significantly in a dose-dependent manner. At 80 μM, Oxo increased LR clustering by 65.7 ± 9.4% ($P < 0.05$, $n = 5$). This Oxo-induced LR clustering effect was abolished by LR disruptors, MCD and filipin, respectively. Des, a selective inhibitor of ASMase, also inhibited this Oxo-induced LR clustering.

Oxo-induced FRET between CD38 and LR component, GM_1. FRET was detected by FITC-labeled anti-CD38 antibody and TRITC-labeled CTX. As shown in Fig. 2*A*, *top*, the green image showed the FITC-labeled anti-CD38 antibody, whereas the red image showed a labeling of GM_1 by TRITC-CTX. The overlaid image mainly showed colocalization, but a subtraction of pre- from postimage on FITC image represents FRET in that we used an acceptor (TRITC) bleaching protocol. In this protocol, TRITC was bleached, and therefore the normally weakened FITC signal due to energy transferring into neighbor molecules could be enhanced. The increase in the FITC-labeled CD38 signal indicates the increase of FRET efficiency, which was derived from the blockade of acceptation of photons by TRITC (bleached). Under control conditions, when two images were overlaid, there was no yellow spots or patches detected. When CAMs were stimulated by Oxo, yellow spots were seen, which represent a colocalization of GM_1 and CD38 (*right*). The green fluorescence intensity of FITC-anti-CD38 antibody (*middle*) increased after the acceptor of TRITC labeling CTX was bleached during Oxo stimulation, whereas the red fluorescence intensity of TRITC labeling CTX almost disappeared due to bleaching. Under this condition, there was no yellow spot detectable in the overlaid image. Figure 2*A*, *bottom*, showed a subtracted image between the pre- and

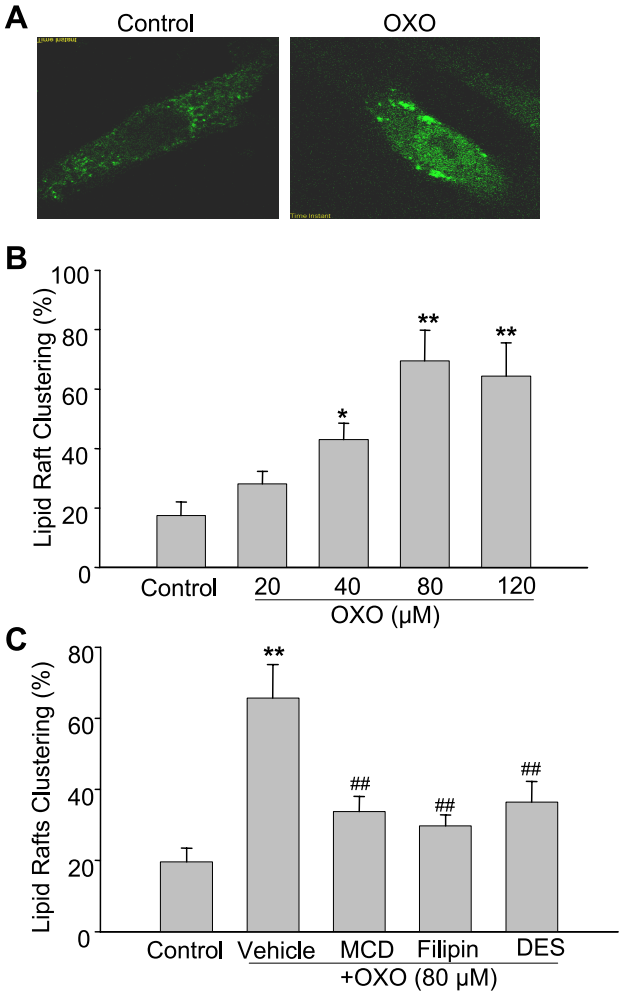

Fig. 1. Oxotremorine (Oxo)-induced lipid-raft (LR) clustering in coronary arterial myocytes (CAMs) membrane in the absence or presence different LR disruptors. *A*: representative images of control and Oxo-stimulated CAMs stained with Al488-cholera toxin B (CTXB). *B*: CAMs were stimulated with different doses of muscarinic type 1 (M_1) receptor agonist, Oxo (20–120 μM) for 15 min to induce LR clustering. *C*: CAMs were stimulated with Oxo (80 μM, 15 min) before and after pretreatment with LR disruptors, methyl-β-cyclodextrin (MCD; 100 μM), filipin (1 μg), or with a selective acid sphingomyelinase (ASMase) inhibitor, desipramine (Des, 10 μM) for 20 min. Shown is the percentage of cells displaying LR clustering. Values presented are means ± SE ($n = 5$ experiments with analysis from more than 1,000 cells). *$P < 0.05$ and **$P < 0.01$ vs. control; ##$P < 0.01$ vs. Oxo-treated group.

postacceptor bleaching, and the blue color intensity represented increased FITC fluorescence due to FRET. Figure 2*B* showed the summarized results of FRET analysis. When compared with control (5.3 ± 0.9%), the efficiency of FRET in the Oxo-treated group of CAMs increased significantly to 15.5 ± 1.9% ($P < 0.01$, $n = 5$). When a same molecule of the cells (CD38) was stained by FITC-labeled primary antibody followed by TRITC-labeled secondary antibody and subjected to FRET protocol, a maximal FRET efficiency was 25% (data not shown). Pretreatment with LR disruptors, MCD or filipin, decreased the FRET efficiency remarkably. In addition, FRET efficiency was also inhibited by Des, an ASMase inhibitor (Fig. 2*B*).

CD38 aggregation in isolated LR fractions. By Western blot analysis, the expression of flotillin-1, a LR specific marker, was primarily found in the fractions between the 5% and 30% gradients, which was referred to LR fractions previously (27). As shown in Fig. 3, the ratio of CD38 levels in LR fractions to those in other fractions were summarized, because their clustering in LR fractions of cell membrane, rather than increase in expression, is comparable. CD38 could be detected in most of the membrane fractions from CAMs under control conditions. There was a marked increase in CD38 protein in LR fractions when these cells were stimulated by Oxo. However, when the cells were pretreated by MCD, filipin, or Des, a Oxo-induced increase in CD38 in LR fractions was significantly blocked.

Contribution of ceramide and ASMase to Oxo-induced LR clustering. To examine whether ASMase/ceramide is involved in Oxo-induced LR clustering and whether Oxo-induced LR clustering forms ceramide-enriched macrodomains, we stained CAMs with Alexa488-CTX and Texas red-conjugated anti-ASMase antibody or Cy3-labeled ceramide. As shown in Fig. 4, Oxo stimulation caused an aggregation of both ceramide (Fig. 4*A*) and ASMase (Fig. 4*B*) in LR clusters (colocalized with CTX-labeled GM_1), which were exhibited by yellow dots

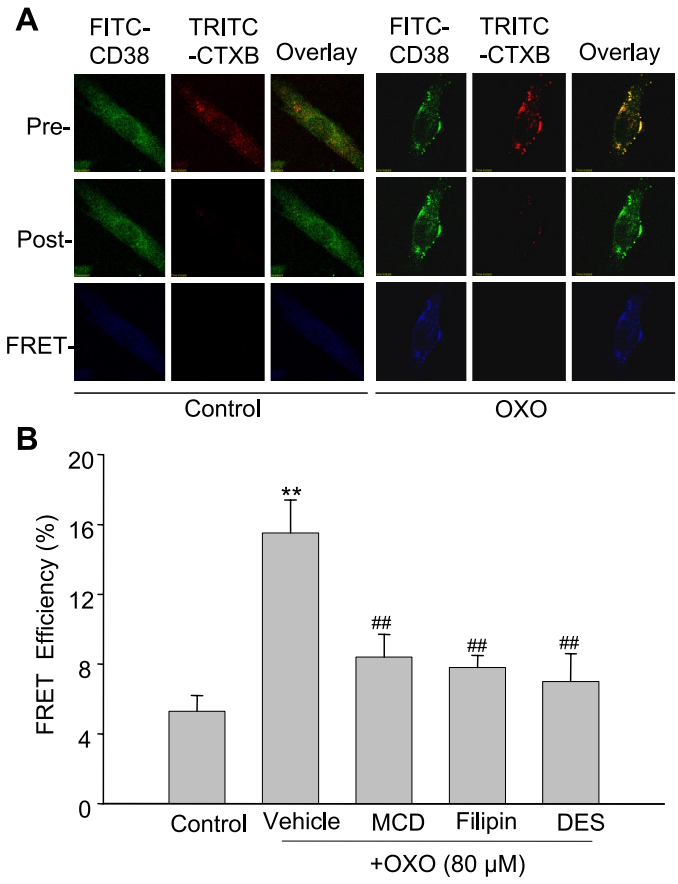

Fig. 2. Fluorescence resonance energy transfer (FRET) between a fluorophore pair, FITC (donor) and tetramethylrhodamine isothiocyanate (TRITC; acceptor) labeled anti-CD38 antibody and LR component, GM_1 binder, CTXB, respectively. Acceptor (TRITC) bleaching protocol was applied to detect the FRET efficiency. *A*: typical images depicting FRET between FITC-conjugated anti-CD38 antibody and TRITC-conjugated CTXB in a control and Oxo-treated CAM, respectively. *B*: means ± SE of FRET efficiency from 5 experiments. Oxo was found to increase the FRET efficiency, and LR disruptors, MCD (100 μM), filipin (1 μg) or ASMase inhibitor Des (10 μM) attenuated Oxo-induced increase in FRET efficiency. **$P < 0.01$ vs. control; ##$P < 0.01$ vs. Oxo-treated group.

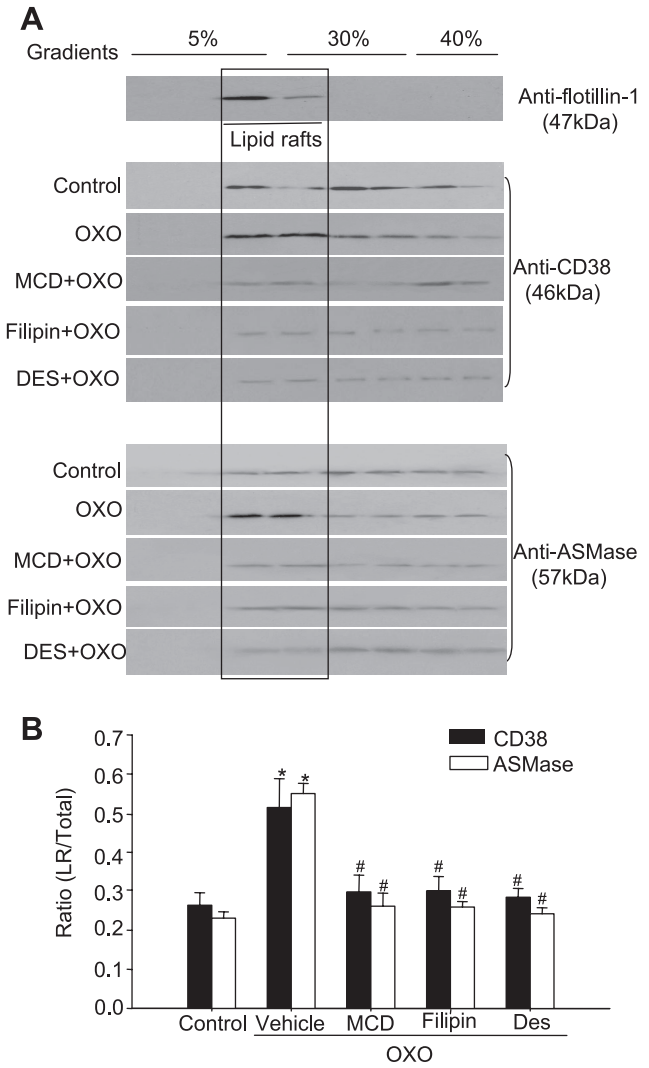

Fig. 3. Western blot analysis of CD38 and ASMase in LR fractions isolated from CAMs stimulated by Oxo. *A*: CAMs were treated with Oxo (80 μM, 15 min) alone or with 20-min pretreatment of MCD (100 μM), filipin (1 μg), or Des (10 μM). Fractions between 5% and 30% gradients were designated as LRs as indicated by the marker protein flotillin-1. The blot pattern for CD38 and ASMase represents 5 individual experiments. *B*: quantified data of the ratio of CD38 or ASMase in LR fraction to that of total in each membrane blot (LR/Total). It was found that Oxo stimulated both CD38 and ASMase aggregation into LR fractions, which was significantly attenuated by LR disruptors and ASMase inhibitors. *$P < 0.05$ vs. control; #$P > 0.05$ vs. control ($n = 5$ experiments).

or patches (*right*). When these cells were pretreated by either MCD or filipin, both CTX clusters (Alexa488 green fluorescence) and aggregated ASMase (Texas red fluorescence) or ceramide (Cy3 fluorescence) were no longer observed. Correspondingly, in isolated LR fractions, ASMase was found to be increased in CAMs treated with Oxo, whereas in other fractions, ASMase contents remained unchanged or reduced. However, in the presence of LR disruptors, MCD or ASMase inhibitor, Des, this redistribution of ASMase induced by Oxo was abolished (Fig. 3).

To further confirm whether ASMase is involved in Oxo-induced LR clustering, we directly measured ASMase activity in CAMs. As shown in Fig. 5*A*, Oxo treatment of CAMs for 15 min markedly increased ASMase activity in CAMs, which was substantially inhibited by ASMase inhibition with Des. However, LR disruptors, MCD or filipin, only had minimal inhibitory effect on Oxo-induced enhancement of ASMase activity, suggesting that ASMase activation may precede LR clustering.

Role of ceramide-enriched lipid platforms with CD38 in Oxo-induced increase in ADP-ribosylcyclase activity in CAMs. To explore the functional significance of ceramide-enriched lipid platforms with CD38 in CAMs, we directly observed the Oxo-induced increase in CD38 activity by HPLC in these cells before and after a pretreatment with LR disruptors, MCD or ASMase inhibitor, Des. As shown in Fig. 5*B*, the conversion rate of β-NGD to cGDPR was 43.1 ± 1.9 under control conditions. When cells were incubated with Oxo, the rate was increased significantly (57.6 ± 3.9). Pretreatment of CAMs with ADP-ribosylcyclase inhibitor, Nicot, significantly inhibited Oxo-induced production of cADPR. MCD and filipin also inhibited the effects of Oxo significantly.

Association of ceramide-enriched lipid-CD38 platforms with Oxo-induced intracellular Ca^{2+} release in CAMs. To further determine the role of ceramide-enriched lipid-CD38 platforms in the regulation of intracellular Ca^{2+} release, we examined Oxo-induced intracellular Ca^{2+} release in CAMs under control conditions and when they were treated with LR disruptors, MCD or filipin, and ASMase inhibitor, Des. In Fig. 6*A*, typical microscopic digitalized signal plots of Ca^{2+} release within CAMs bathed in Ca^{2+}-free solution are presented. It is clear that in the presence of 8-Br-cADPR (a cADPR antagonist), Des, MCD or filipin, Oxo-induced Ca^{2+} release in CAMs was significantly reduced compared with Oxo

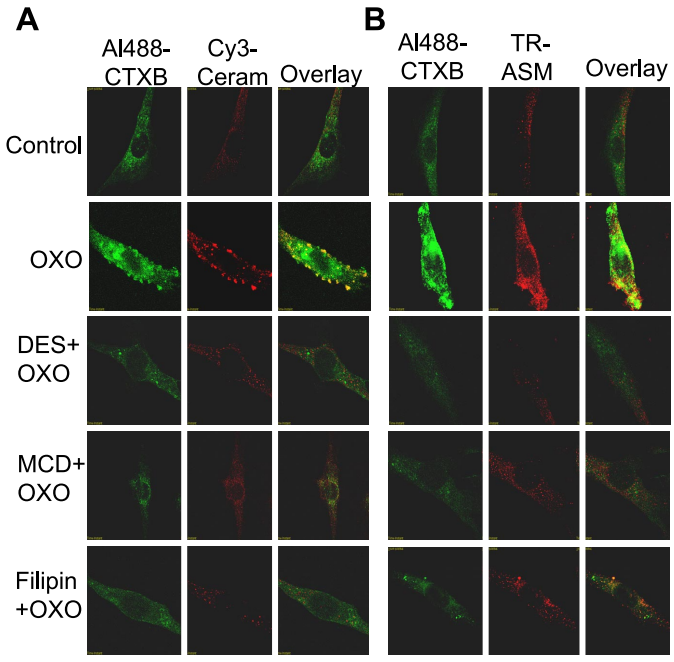

Fig. 4. Confocal microscopic analysis of ceramide (Ceram) and ASMase colocalization in LR clusters in CAMs. *A*: the cells stained with Texas red (TR)-conjugated anti-ASMase antibody and Alexa488 (Al488)-CTXB. *B*: the cells stained with Cy3-conjugated anti-ceramide antibody and Alexa488-CTXB. Ceramide and ASMase were found to be colocalized with LR marker when CAMs were stimulated by Oxo. This Oxo-induced colocalization can be blocked by pretreatment of the cells with LR disruptors (MCD or filipin) and ASMase inhibitor, Des.

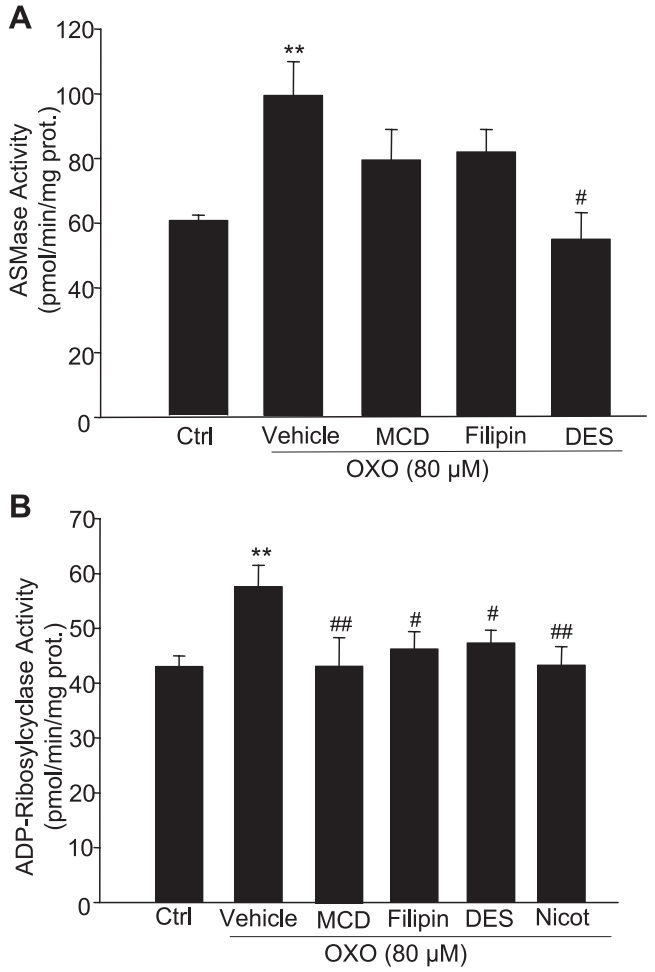

Fig. 5. Effects of Oxo on ASMase and ADP-ribosylcyclase activity in CAMs in the absence or presence of LR disruptors. *A*: summarized ASMase activity of CAMs treated with Oxo (80 μM, 15 min) alone or with 20-min pretreatment of MCD (100 μM), filipin (1 μg), or Des (10 μM). Values are means ± SE of 5 experiments. Prot, protein. $^{**}P < 0.01$ vs. control; $^{\#}P < 0.05$ vs. Oxo-treated group. *B*: summarized ADP-ribosylcyclase activity of CAMs treated with Oxo (80 μM, 15 min) alone or with 20-min pretreatment of MCD (100 μM), filipin (1 μg), or nicotinamide (Nicot; 6 mM) or Des (10 μM). Values are means ± SE from 5 experiments. $^{**}P < 0.01$ vs. control (Ctrl); $^{\#}P < 0.05$ vs. Oxo-treated group; $^{\#\#}P < 0.01$.

stimulation alone. Calculated Ca^{2+} concentrations under different conditions are presented in Fig. 6*B*. In response to Oxo stimulation, intracellular Ca^{2+} concentration increased from 149.8 ± 32.7 to 495.0 ± 130.6 nM in CAMs. This Oxo-induced increase in intracellular Ca^{2+} levels could be attenuated or blocked by inhibition of LR clustering or formation of ceramide-enriched platforms either with LR disruptors or ASMase inhibitor.

Role of ceramide-enriched lipid platforms with CD38 in Oxo-induced vasoconstriction. Consistent with our previous reports (11, 43), we found that in the presence of Nicot or 8-Br-cADPR, the Oxo-induced contraction of small coronary arteries was significantly attenuated. The maximal contraction decreased from 47.2 ± 6.8% to 21.1 ± 4.2% or 27.3 ± 4.8%, respectively ($n = 5$). In the presence of MCD or filipin, the Oxo-induced contraction was also significantly reduced to a very similar extent to that induced by Nicot or 8-Br-cADPR. When ASMase inhibitor, Des, was used to treat the coronary arteries, the maximal contraction induced by Oxo decreased from 47.2 ± 6.8% to 26.5 ± 3.9% ($n = 5$) (Fig. 6*C*).

DISCUSSION

The main findings of the present study are that *1*) Oxo induced LR clustering in CAMs as shown by the formation of larger membrane LR patches as detected by confocal microscopy; *2*) Oxo induced an aggregation of CD38 in LR clusters with enriched ceramide, which resulted in the increased activity of CD38 as ADP-ribosylcyclase, and disruption of LRs inhibited the effects of Oxo on this enzyme activity; and *3*) blockade of ASMase/ceramide inhibited Oxo-induced LR clustering and consequent CD38 activation and cADPR pro-

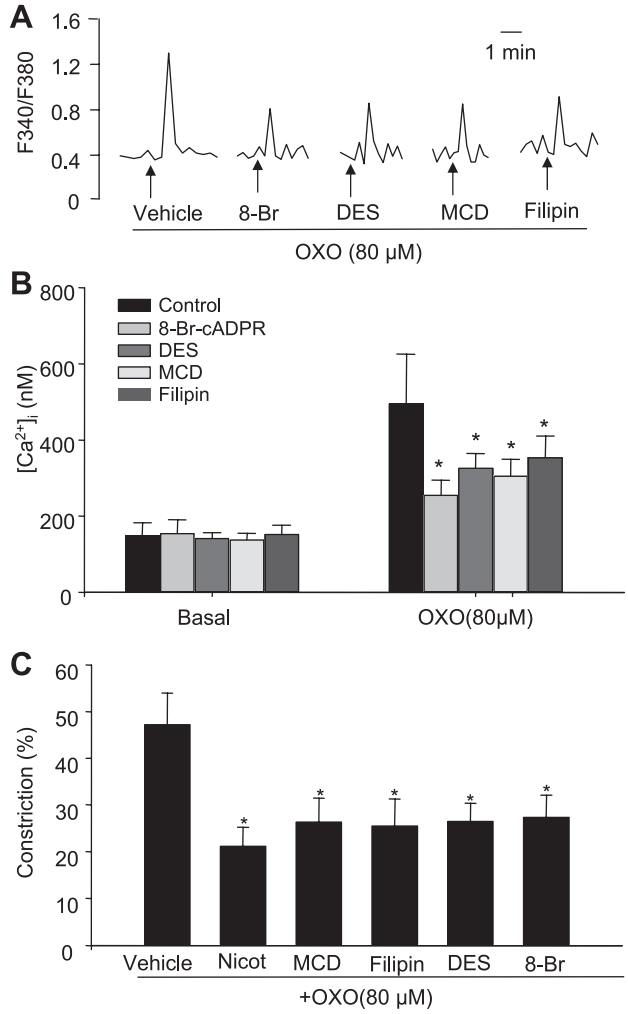

Fig. 6. Association of ceramide-enriched lipid-CD38 platforms with Oxo-induced intracellular Ca^{2+} release in CAMs and vessel constriction in small coronary arteries. *A*: representative recording of fura-2 Ca^{2+} signals by a high speed wavelength switch microscopic imaging system. F340/F380, emission fluorescence ratio with excitation at 340 and 380 nm. *B*: summarized intracellular free Ca^{2+} level in CAMs treated with Oxo (80 μM, 15 min) alone or with 20-min pretreatment of MCD (100 μM), filipin (1 μg), 8-bromo-cADPR (8-Br; 30 μM), or Des (10 μM). Values are means ± SE from 5 experiments. $[Ca^{2+}]_i$, intracellular Ca^{2+} concentration. *C*: summarized data showing the constriction of small coronary arteries treated with Oxo (80 μM, 15 min) alone or with 20 min pretreatment of MCD (100 μM), filipin (1 μg), or Nicot (6 mM) or Des (10 μM). Values are means ± SE of 5 experiments. $^{*}P < 0.05$ vs. Oxo-treated group.

duction, whereby an Oxo-induced increase in intracellular Ca^{2+} release and vasoconstriction was significantly attenuated. These results support our hypothesis that ceramide-enriched LR platforms mediate Oxo-induced transmembrane signaling of CD38 and thereby activate its ADP-ribosylcyclase to produce cADPR in CAMs.

Despite the increasing evidence that cADPR signaling becomes an essential mechanism in the regulation of the intracellular Ca^{2+} level in a variety of mammalian cells (6, 19), so far it remains unknown what mechanism mediates cADPR production in response to various agonists or stimuli and how a transmembrane signaling upon agonist stimulation occurs to activate cADPR producing enzyme and leads to responses of intracellular effectors. Moreover, there is evidence that CD38, a major enzyme producing cADPR in mammalian cells or tissues, is mainly present on the surface of cells serving as an ectoenzyme (1). It is imperative to know how an ectoenzyme could produce a second messenger to mediate intracellular Ca^{2+} signaling as an important function of cADPR. In the present study, we tested a novel hypothesis that LRs may form a signaling platform in vascular smooth muscle cells where CD38 can be aggregated and activated to produce cADPR when these cells are stimulated by agonists. This LRs-mediated transmembrane signaling may represent a novel mechanism initiating cADRP production and subsequent signaling cascade. The rationale of this hypothesis is based on the fact that the LRs may serve as anchoring platforms for organizing components of the signal transduction systems (8, 12, 30) and thereby participate in cellular signaling. In this regard, these LRs are known as specialized membrane microdomains rich of cholesterol and sphingolipids, which act as organizing centers by sequestering specific sets of proteins for different cellular activities such as membrane molecular trafficking and signal transduction (2). In vascular smooth muscle cells, LRs have been demonstrated to play an important role in several cell signaling pathways, such as agonist-induced Ca^{2+} release, phosphorylation of EGF receptor, and activation of RhoA (7, 17, 24). Using confocal microscopic analysis of GM_1 labeling by CTX as a marker of LR clusters, we found that under control conditions, LRs were diffusely distributed throughout the membrane of CAMs and that stimulation of these cells with Oxo resulted in a dose-dependent formation of CTX-positive fluorescent patches, which represented LR clusters or macrodomains. This suggests that LR clustering occurs in arterial smooth muscle cells in response to agonists such as Oxo. Given its well-known signaling role, this LR clustering may be of importance in mediating signal transduction or functional response in these vascular smooth muscles. Indeed, we demonstrated that this LR clustering was coupled to CD38 aggregation, as shown in confocal microscopic colocalization analysis, FRET detection, and membrane flotation of LR fractions. These LR-CD38 complex or membrane platforms may result in CD38 translocation and activation by agonists such as Oxo. To our knowledge, these results for the first time provide direct evidence that LRs are able to be clustered with aggregation of CD38 in vascular smooth muscle cells. In previous studies, this LR-mediated CD38 clustering was also reported in T-cells or B-cells, which participates in the regulation of T-cell or B-cell function by facilitating critical associations or interactions with other signaling molecules such as myosin heavy chain class II, CD9, N-Ras, Akt, Erk, Lck and CD3-ζ (4, 25, 46, 48). However, the regulation of lymphocyte function by LR clustering has not been linked to its function of cADPR production and consequent Ca^{2+} mobilization.

In the present study, we provided further evidence that the aggregation of CD38 via LR clustering is involved in the activation of this enzyme to produce cADPR. By HPLC analysis of cGDPR production as an ADP-ribosyl cyclase activity, Oxo was found to significantly increase the activity of CD38 in CAMs, which was blocked by LR disruptors MCD and filipin. This suggests that LR clustering in these cells importantly contribute to the activation of CD38 as a cADPR-producing enzyme. To further determine the role of LR clustering in cADPR-mediated signaling, we addressed whether the activation of CD38 via LR clustering is attributed to Oxo-induced Ca^{2+} release response in CAMs. It has been reported that CD38 is a crucial pathway mediating Ca^{2+} release, and our previous work also demonstrated that cADPR-mediated Ca^{2+} mobilization represents an important signaling pathway participating in the Ca^{2+} regulation in vascular smooth muscle cells and in the vasoconstrictor response of coronary arteries when M_1 ACh receptor is activated (40). Consistent with these previous studies, the present study found that Oxo induced Ca^{2+} release from the SR in CAMs buffered in Ca^{2+}-free solution and that 8-Br-cADPR, an antagonist of cADPR, could block the action of Oxo. Interestingly, in the presence of LR disruptors, MCD or filipin, Oxo-induced Ca^{2+} release was substantially attenuated. In another series of experiments, we also examined the contribution of this LR clustering with CD38 to the vasoconstrictor response to Oxo. It was found that Oxo induced significant vasoconstriction with a maximal response of $47.2 \pm 6.8\%$ in perfused and pressurized small coronary arteries, which was significantly blocked by the LR disruptor, MCD or filipin. Taken together, these results indicate that LRs and their clustering importantly participate in the regulation of vascular function associated with CD38 activation and cADPR-mediated Ca^{2+} release in coronary arteries. To our knowledge, this represents the first report elucidating the functional association of LR clustering with CD38 activity to produce cADPR in the regulation of intracellular Ca^{2+} level of arterial myocytes and vasomotor response in coronary arteries. Previous studies also demonstrated the formation of LR-CD38 complex in lymphocytes in response to different stimuli (4, 25, 46). However, these studies did not demonstrate the correlation between the production of cADPR and agonist receptor functions when LR clustering occurred, but they assumed that CD38 may serve as a pleiotropic molecule in LR clusters, whose behavior or function is independent from its enzymatic activity in these cells (46). In some other studies, CD38 in LRs has been demonstrated as an interacting membrane molecule to facilitate the formation of different signaling complex in lymphocytes, which activates several different phosphorylation pathways to regulate cell proliferation or apoptosis (7, 48).

It should be noted that although Oxo or M_1 agonist may not be a major regulator of coronary vascular tone under physiological conditions, the use of this compound represents a prototype of agonists that stimulates cADPR production and induces vasoconstriction of bovine coronary arteries because bovine coronary arteries did not respond to angiotensin II or norepinephrine to produce vasoconstriction based on our experience working on this type of arteries for more than 10 years. Another comparable vasoconstrictor in these arteries is

to thromboxane A_2 mimetic, U-46619, a commonly used agonist in these bovine arteries, but this compound produces vasoconstriction through Ins(1,4,5)P_3 independent of LRs. With respect to agonists or stimuli that use cADPR as second messengers, recent studies have demonstrated that there are Oxo in smooth muscle cells, cholecystokinin in pancreatic acinar cells, glucose in pancreatic β-cells, physiological contact or fertilization in the eggs, histamine and oxytoxin in myometrial cells, and thrombin in platelets. Based our results in using Oxo, an agonist producing comparable vasoconstriction to Ins(1,4,5)P_3 stimulator, we believe the LR-mediated activation of ADP-ribosylcyclase demonstrated in the present study is mainly attributed to this type of agonists. This LR-signaling mechanism may not be used by other Ca^{2+} regulatory pathways.

To explore the mechanism by which Oxo induces the formation of LR clusters with CD38 in CAMs, we tested a hypothesis that ASMase or ceramide plays a critical role in Oxo-induced LR clustering and thereby contributes to corresponding functional changes in CAMs or coronary arterial smooth muscle. There is considerable evidence that rapid activation and translocation of ASMase into cell membrane trigger or facilitate the formation of LR clusters in response to different stimuli (22). Recent studies in our laboratory have shown that lysosome-associated vesicle transportation or trafficking of ASMase from intracellular compartments to cell membrane is a prerequisite for ASMase activation in the process of LR clustering in endothelial cells (18). This ASMase translocated into cell membrane hydrolyzes SM to produce ceramide and leads to the formation of ceramide-enriched macrodomains or LR platforms, which cluster or recruit some receptors or signaling molecules (22). The present study provided several lines of evidence that this translocated ASMase and consequently produced ceramide are present in LR clusters with CD38 in CAMs and that ceramide production from ASMase importantly contributes to the formation and function of LR clusters with CD38. First, under stimulation of Oxo, ASMase and ceramide were found to be aggregated in LR clusters with CD38, as shown by the colocalization of GM_1 labeled by Alexa-CTX and ASMase, and ceramide labeled by Texas red-conjugated anti-ASMase antibody and Cy3-conjugated anti-ceramide antibody, respectively. Second, by membrane floatation, ASMase was found to be enriched in LR fractions and ASMase activity significantly increased in these fractions. The ASMase inhibitor, Des, could block these effects, but LR disruptors did not have obvious effects on Oxo-induced ASMase activation. These results suggest that ASMase enrichment and activation are involved in Oxo-induced LR clustering, and even ASMase activation precedes the LR clustering because the LR disruptors could not block the increased ASMase activity stimulated by Oxo. Third, a biochemical analysis demonstrated that ASMase inhibition by Des significantly blocked ADP-ribosylcyclase activity of CD38 in CAMs, indicating that ASMase importantly contributes to CD38 activation to produce cADPR. Fourth, functional studies by the measuring intracellular Ca^{2+} level in CAMs and the vasoconstrictor response of coronary arteries to Oxo provided evidence that ASMase inhibition attenuated the effect of Oxo-induced Ca^{2+} activation and vasoconstriction in these arteries. All these results support the view that ASMase and its product ceramide pathway play a crucial role in Oxo-induced LR clustering and consequently CD38 activation and that the formation of these ceramide-enriched lipid platforms importantly participate in the CD38-cADPR-mediated signaling upon activation of M_1 receptor in CAMs.

Oxo or some other agonists may produce Ca^{2+} release and consequent vasoconstriction through several pathways such as activation of plasma membrane Ca^{2+} channels and Ins(1,4,5)P_3 production and resulting intracellular Ca^{2+} release. However, these two pathways will be blocked by using a Ca^{2+}-free bath solution in our Ca^{2+} assay and vasoreactivity studies as a routine in such studies. Under this condition, Ca^{2+} influx is blocked and therefore its role in mediating Oxo action was minimized. In addition, it was reported that when cells are bathed in Ca^{2+} free solution, PLC failed to respond to any stimulus to produce Ins(1,4,5)P_3 (34). Therefore, there was only a minimal action of Ins(1,4,5)P_3 in such preparations. However, our results did not exclude the action of Ca^{2+} influx or Ins(1,4,5)P_3 in the action of Oxo or other agonists under other conditions.

There was a concern regarding alternative pathways for cADPR production. It has been demonstrated that a soluble protein, ADP-ribosyl cyclase and its membrane-bound homologous CD38 and CD157, are involved in the production of cADPR with the substrate NAD^+ by a cyclizing reaction (9, 23), which has been shown in a variety of cells and tissues such as sea urchin eggs, pancreatic acinar cells, human T lymphocytes, rat brain, and rat smooth muscle cells. Over the last 10 years, we have demonstrated that this cADPR-mediated Ca^{2+} signaling is present in cardiovascular tissues such as the myocardium, renal microvessel, and coronary arteries (10, 32, 38). We also demonstrated that ADP-ribosylcyclases activity is primarily derived from CD38 (a GPI-anchored protein) in coronary arterial smooth muscle. In addition, other studies reported that CD38 internalization is of importance in mediating cADP-ribose production in cell cytosol (14, 47). Therefore, based on current understanding, the high level of ADP-ribosylcyclase activity to convert NAD^+ to cADPR may be associated with the internalization of a membrane-bound enzyme, although there may be some unidentified pathways. One such unidentified pathway was reported recently in myometrial cells, which possesses ADP-ribosylcyclase activity to produce cADPR and NAADP independent of CD38 and CD157 (28). In addition, CD38-mediated cADPR has been reported to be enhanced by protein kinase A and cAMP-regulated guanine nucleotide exchange factor II (20). It seems that different type of cells may use different enzymatic pathways to produce cADPR. This CD38-independent pathway for cADPR production has not yet been demonstrated in vascular smooth muscle cells. However, our results in the present studies did not exclude the role of this CD38-independent pathway in mediating vascular reactivity under other conditions or when these cells are stimulated by other agonists.

In summary, the present study demonstrated that Oxo stimulated LR clustering in CAMs and that a membrane signaling complex or platforms could be formed by LR clustering. This LR clustering or formation of signaling platforms importantly participates in Ca^{2+} transient response of CAMs to Oxo and corresponding coronary arterial constriction. The Oxo-induced formation of LR signaling platform with CD38 as a complex was dependent on the enrichment and activation of ASMase and consequent production of ceramide. Therefore, it is the

ceramide-enriched macrodomain or lipid platforms that mediate the action of Oxo in mediating CD38 translocation and activation, thereby producing cADPR to induce Ca^{2+} release from the SR of CAMs. This LR clustering and consequent formation of signaling platforms may represent an important mechanism that is implicated in CD38/cADPR-mediated signaling in coronary arterial smooth muscle in response to vasoactive agonists such as Oxo.

GRANTS

This study was supported by National Institutes of Health Grants HL-57244, HL-75316, and DK-54927.

REFERENCES

1. **An NH, Han MK, Um C, Park BH, Park BJ, Kim HK, Kim UH.** Significance of ecto-cyclase activity of CD38 in insulin secretion of mouse pancreatic islet cells. *Biochem Biophys Res Commun* 282: 781–786, 2001.
2. **Bollinger CR, Teichgraber V, Gulbins E.** Ceramide-enriched membrane domains. *Biochim Biophys Acta* 1746: 284–294, 2005.
3. **Chen YF, Zhang AY, Zou AP, Campbell WB, Li PL.** Protein methylation activates reconstituted ryanodine receptor-ca release channels from coronary artery myocytes. *J Vasc Res* 41: 229–240, 2004.
4. **Deaglio S, Vaisitti T, Billington R, Bergui L, Omede P, Genazzani AA, Malavasi F.** CD38/CD19: a lipid raft-dependent signaling complex in human B cells. *Blood* 109: 5390–5398, 2007.
5. **Fellner SK, Arendshorst WJ.** Angiotensin II Ca^{2+} signaling in rat afferent arterioles: stimulation of cyclic ADP ribose and IP_3 pathways. *Am J Physiol Renal Physiol* 288: F785–F791, 2005.
6. **Fliegert R, Gasser A, Guse AH.** Regulation of calcium signalling by adenine-based second messengers. *Biochem Soc Trans* 35: 109–114, 2007.
7. **Fritz N, Macrez N, Mironneau J, Jeyakumar LH, Fleischer S, Morel JL.** Ryanodine receptor subtype 2 encodes Ca^{2+} oscillations activated by acetylcholine via the M_2 muscarinic receptor/cADP-ribose signalling pathway in duodenum myocytes. *J Cell Sci* 118: 2261–2270, 2005.
8. **Furne C, Corset V, Herincs Z, Cahuzac N, Hueber AO, Mehlen P.** The dependence receptor DCC requires lipid raft localization for cell death signaling. *Proc Natl Acad Sci USA* 103: 4128–4133, 2006.
9. **Galione A.** Cyclic ADP-ribose: a new way to control calcium. *Science* 259: 325–326, 1993.
10. **Ge ZD, Li PL, Chen YF, Gross GJ, Zou AP.** Myocardial ischemia and reperfusion reduce the levels of cyclic ADP-ribose in rat myocardium. *Basic Res Cardiol* 97: 312–319, 2002.
11. **Ge ZD, Zhang DX, Chen YF, Yi FX, Zou AP, Campbell WB, Li PL.** Cyclic ADP-ribose contributes to contraction and Ca^{2+} release by M_1 muscarinic receptor activation in coronary arterial smooth muscle. *J Vasc Res* 40: 28–36, 2003.
12. **Gupta N, DeFranco AL.** Visualizing lipid raft dynamics and early signaling events during antigen receptor-mediated B-lymphocyte activation. *Mol Biol Cell* 14: 432–444, 2003.
13. **Guse AH, da Silva CP, Berg I, Skapenko AL, Weber K, Heyer P, Hohenegger M, Ashamu GA, Schulze-Koops H, Potter BV, Mayr GW.** Regulation of calcium signalling in T lymphocytes by the second messenger cyclic ADP-ribose. *Nature* 398: 70–73, 1999.
14. **Han MK, Kim SJ, Park YR, Shin YM, Park HJ, Park KJ, Park KH, Kim HK, Jang SI, An NH, Kim UH.** Antidiabetic effect of a prodrug of cysteine, L-2-oxothiazolidine-4-carboxylic acid, through CD38 dimerization and internalization. *J Biol Chem* 277: 5315–5321, 2002.
15. **Herincs Z, Corset V, Cahuzac N, Furne C, Castellani V, Hueber AO, Mehlen P.** DCC association with lipid rafts is required for netrin-1-mediated axon guidance. *J Cell Sci* 118: 1687–1692, 2005.
16. **Horejsi V.** The roles of membrane microdomains (rafts) in T cell activation. *Immunol Rev* 191: 148–164, 2003.
17. **Hunter I, Nixon GF.** Spatial compartmentalization of tumor necrosis factor (TNF) receptor 1-dependent signaling pathways in human airway smooth muscle cells. Lipid rafts are essential for TNF-alpha-mediated activation of RhoA but dispensable for the activation of the NF-kappaB and MAPK pathways. *J Biol Chem* 281: 34705–34715, 2006.
18. **Jin S, Yi F, Li PL.** Contribution of lysosomal vesicles to the formation of lipid raft redox signaling platforms in endothelial cells. *Antioxid Redox Signal* 9: 1417–1426, 2007.
19. **Jude JA, Wylam ME, Walseth TF, Kannan MS.** Calcium signaling in airway smooth muscle. *Proc Am Thorac Soc* 5: 15–22, 2008.
20. **Kim BJ, Park KH, Yim CY, Takasawa S, Okamoto H, Im MJ, Kim UH.** Generation of nicotinic acid adenine dinucleotide phosphate and cyclic ADP-ribose by glucagon-like peptide-1 evokes Ca^{2+} signal that is essential for insulin secretion in mouse pancreatic islets. *Diabetes* 57: 868–878, 2008.
21. **Kip SN, Smelter M, Iyanoye A, Chini EN, Prakash YS, Pabelick CM, Sieck GC.** Agonist-induced cyclic ADP ribose production in airway smooth muscle. *Arch Biochem Biophys* 452: 102–107, 2006.
22. **Lacour S, Hammann A, Grazide S, Lagadic-Gossmann D, Athias A, Sergent O, Laurent G, Gambert P, Solary E, Dimanche-Boitrel MT.** Cisplatin-induced CD95 redistribution into membrane lipid rafts of HT29 human colon cancer cells. *Cancer Res* 64: 3593–3598, 2004.
23. **Lee HC.** Mechanisms of calcium signaling by cyclic ADP-ribose and NAADP. *Physiol Rev* 77: 1133–1164, 1997.
24. **Liu YT, Song L, Templeton DM.** Heparin suppresses lipid raft-mediated signaling and ligand-independent EGF receptor activation. *J Cell Physiol* 211: 205–212, 2007.
25. **Munoz P, Navarro MD, Pavon EJ, Salmeron J, Malavasi F, Sancho J, Zubiaur M.** CD38 signaling in T cells is initiated within a subset of membrane rafts containing Lck and the CD3-zeta subunit of the T cell antigen receptor. *J Biol Chem* 278: 50791–50802, 2003.
26. **Noda M, Yasuda S, Okada M, Higashida H, Shimada A, Iwata N, Ozaki N, Nishikawa K, Shirasawa S, Uchida M, Aoki S, Wada K.** Recombinant human serotonin 5A receptors stably expressed in C6 glioma cells couple to multiple signal transduction pathways. *J Neurochem* 84: 222–232, 2003.
27. **Shao D, Segal AW, Dekker LV.** Lipid rafts determine efficiency of NADPH oxidase activation in neutrophils. *FEBS Lett* 550: 101–106, 2003.
28. **Soares S, Thompson M, White T, Isbell A, Yamasaki M, Prakash Y, Lund FE, Galione A, Chini EN.** NAADP as a second messenger: neither CD38 nor base-exchange reaction are necessary for in vivo generation of NAADP in myometrial cells. *Am J Physiol Cell Physiol* 292: C227–C239, 2007.
29. **Solomon JC, Sharma K, Wei LX, Fujita T, Shi YF.** A novel role for sphingolipid intermediates in activation-induced cell death in T cells. *Cell Death Differ* 10: 193–202, 2003.
30. **Sprenger RR, Fontijn RD, van Marle J, Pannekoek H, Horrevoets AJ.** Spatial segregation of transport and signalling functions between human endothelial caveolae and lipid raft proteomes. *Biochem J* 400: 401–410, 2006.
31. **Sturmey RG, O'Toole PJ, Leese HJ.** Fluorescence resonance energy transfer analysis of mitochondrial:lipid association in the porcine oocyte. *Reproduction* 132: 829–837, 2006.
32. **Teggatz EG, Zhang G, Zhang AY, Yi F, Li N, Zou AP, Li PL.** Role of cyclic ADP-ribose in Ca^{2+}-induced Ca^{2+} release and vasoconstriction in small renal arteries. *Microvasc Res* 70: 65–75, 2005.
33. **Testai FD, Landek MA, Dawson G.** Regulation of sphingomyelinases in cells of the oligodendrocyte lineage. *J Neurosci Res* 75: 66–74, 2004.
34. **Thore S, Dyachok O, Gylfe E, Tengholm A.** Feedback activation of phospholipase C via intracellular mobilization and store-operated influx of Ca^{2+} in insulin-secreting beta-cells. *J Cell Sci* 118: 4463–4471, 2005.
35. **Trubiani O, Guarnieri S, Orciani M, Salvolini E, Di Primio R.** Sphingolipid microdomains mediate CD38 internalization: topography of the endocytosis. *Int J Immunopathol Pharmacol* 17: 293–300, 2004.
36. **Van Munster EB, Kremers GJ, Adjobo-Hermans MJ, Gadella TW Jr.** Fluorescence resonance energy transfer (FRET) measurement by gradual acceptor photobleaching. *J Microsc* 218: 253–262, 2005.
37. **Young GS, Jacobson EL, Kirkland JB.** Water maze performance in young male Long-Evans rats is inversely affected by dietary intakes of niacin and may be linked to levels of the NAD^+ metabolite cADPR. *J Nutr* 137: 1050–1057, 2007.
38. **Zhang AY, Li PL.** Vascular physiology of a Ca^{2+} mobilizing second messenger-cyclic ADP-ribose. *J Cell Mol Med* 10: 407–422, 2006.
39. **Zhang AY, Yi F, Jin S, Xia M, Chen QZ, Gulbins E, Li PL.** Acid sphingomyelinase and its redox amplification in formation of lipid raft redox signaling platforms in endothelial cells. *Antioxid Redox Signal* 9: 817–828, 2007.
40. **Zhang AY, Yi F, Teggatz EG, Zou AP, Li PL.** Enhanced production and action of cyclic ADP-ribose during oxidative stress in

small bovine coronary arterial smooth muscle. *Microvasc Res* 67: 159–167, 2004.
41. **Zhang AY, Yi F, Zhang G, Gulbins E, Li PL.** Lipid raft clustering and redox signaling platform formation in coronary arterial endothelial cells. *Hypertension* 47: 74–80, 2006.
42. **Zhang DX, Harrison MD, Li PL.** Calcium-induced calcium release and cyclic ADP-ribose-mediated signaling in the myocytes from small coronary arteries. *Microvasc Res* 64: 339–348, 2002.
43. **Zhang F, Jin S, Yi F, Xia M, Dewey WL, Li PL.** Local production of O_2^- by NAD(P)H oxidase in the sarcoplasmic reticulum of coronary arterial myocytes: cADPR-mediated Ca^{2+} regulation. *Cell Signal* 20: 637–644, 2008.
44. **Zhang F, Zhang G, Zhang AY, Koeberl MJ, Wallander E, Li PL.** Production of NAADP and its role in Ca^{2+} mobilization associated with lysosomes in coronary arterial myocytes. *Am J Physiol Heart Circ Physiol* 291: H274–H282, 2006.
45. **Zhang G, Zhang F, Muh R, Yi F, Chalupsky K, Cai H, Li PL.** Autocrine/paracrine pattern of superoxide production through NAD(P)H oxidase in coronary arterial myocytes. *Am J Physiol Heart Circ Physiol* 292: H483–H495, 2007.
46. **Zilber MT, Setterblad N, Vasselon T, Doliger C, Charron D, Mooney N, Gelin C.** MHC class II/CD38/CD9: a lipid-raft-dependent signaling complex in human monocytes. *Blood* 106: 3074–3081, 2005.
47. **Zocchi E, Usai C, Guida L, Franco L, Bruzzone S, Passalacqua M, De Flora A.** Ligand-induced internalization of CD38 results in intracellular Ca^{2+} mobilization: role of NAD^+ transport across cell membranes. *FASEB J* 13: 273–283, 1999.
48. **Zubiaur M, Fernandez O, Ferrero E, Salmeron J, Malissen B, Malavasi F, Sancho J.** CD38 is associated with lipid rafts and upon receptor stimulation leads to Akt/protein kinase B and Erk activation in the absence of the CD3-zeta immune receptor tyrosine-based activation motifs. *J Biol Chem* 277: 13–22, 2002.